The triple integral was performed numerically, with limits of integration $3\times10^2\leq N\leq3\times10^7$ and $0\leq r\leq700$ m.

The function $f(N)dN$ was obtained by differentiating an integral spectrum given by Greisen[7] and then increasing the normalization by 16% to account for the net effect of the altitude above sea level and the material above each scintillator.

The functional form for $g_e(r)$ was that used by the air shower group at Cornell, and is

$$g_e(r)=4.11Nr^{-0.75}(r+82)^{-3.25}(610+r) \text{ particles/m}^2.$$

Values for $g_n(r)$ were taken from the work at Sydney.[2]

$A_m$ was obtained as the mean spectrometer sensitive area by calculating from geometry the sensitive area as a function of zenith angle and integrating this over zenith angle, weighting with the zenith angle distribution of shower arrivals, also obtained by the Cornell group. It turns out that $C^i$ is very nearly linear in $A_m$ so that negligible error is introduced by using a mean value. $A_n$ was estimated by comparing the number of events in which interactions occurred in the spectrometer with the number in which no interaction was observed, for showers whose cores landed close enough to the spectrometer to make the density of muons and nuclear-active particles roughly equal.

### ACKNOWLEDGMENTS

The authors wish to thank Dr. John Delvaille and Dr. Francis Kendziorski who designed and operated the air shower array, and Dr. William Pak who shared in the operation of the spectrometer.

PHYSICAL REVIEW VOLUME 124, NUMBER 6 DECEMBER 15, 1961

# $\pi^-p$ Interactions at 224 Mev*

J. Deahl,† M. Derrick,‡ J. Fetkovich, T. Fields, and G. B. Yodh§
*Department of Physics, Carnegie Institute of Technology, Pittsburgh, Pennsylvania*

(Received August 11, 1961)

Interactions of 224-Mev negative pions with protons were investigated using a 15-cm hydrogen bubble chamber in a 13-kgauss field. Seventeen hundred elastic scatterings were analyzed yielding a cross section of 16.0±0.8 mb for this process. No evidence for powers of $\cos\theta$ higher than two was observed in the angular distribution. The charge-exchange cross section, based on 1200 events was 34.4±1.9 mb. The results of a random-search phase-shift analysis, using these data in conjunction with earlier $\pi^+$-$p$ elastic scattering results and recoil proton polarization measurements ($\pi^-$-$p$), are reported. A search for pion production yielded three events of the type $\pi^-+p\rightarrow\pi^-+\pi^+ +n$ corresponding to a cross section of $\sim30\,\mu$b. No events of the type $\pi^-+p\rightarrow\pi^-+\pi^0+p$ were observed.

## INTRODUCTION

THE main features of pion-proton scattering at energies less than about 300 Mev are in good accord with the results of the Chew-Low-Wick static theory and with the forward-scattering dispersion relations. Experimental and theoretical knowledge concerning the finer aspects of the $\pi$-$p$ interaction, such as $s$-wave phase shifts, the small $p$-wave phase shifts, $d$-wave phase shifts, and inelastic scattering processes, is in a much less certain state.

The present experiment was undertaken to obtain further data on some of the latter phenomena. The experimental method involved the observation of several thousand interactions of 225-Mev negative pions in a hydrogen bubble chamber. It was anticipated that this technique would permit a statistical accuracy comparable to that of existing counter data, but would not be susceptible to systematic errors of the same types as with counter techniques. Furthermore, rare processes, such as inelastic scattering with the production of an additional pion, can be readily identified with the bubble chamber technique.

In analyzing the data of this experiment, the following reactions were considered:

| | | |
|---|---|---|
| (1) | $\pi^-+p\rightarrow\pi^-+p$, | Elastic |
| (2) | $\rightarrow\pi^0+n$, | Charge exchange |
| (3) | $\rightarrow\gamma+n$, | Radiative absorption |
| (4) | $\rightarrow\pi^-+p+\gamma$, | Bremsstrahlung |
| (5) | $\rightarrow\pi^-+\pi^+ +n$, | $\pi^+$ production |
| (6) | $\rightarrow\pi^-+\pi^0+p$, | $\pi^0$ production |
| (7) | $\rightarrow\pi^0+\pi^0+n$. | |

* This work supported in part by the U. S. Atomic Energy Commission. A thesis based on this work has been submitted to the Carnegie Institute of Technology by J. Deahl in partial fulfillment of the requirements for the degree of Doctor of Philosophy. Preliminary accounts of the work have been given: J. Deahl, M. Derrick, J. Fetkovich, T. Fields, and G. B. Yodh, Bull. Am. Phys. Soc. 5, 71 (1960); J. Deahl, M. Derrick, J. Fetkovich, T. Fields, and G. B. Yodh, *Proceedings of the 1960 Annual International Conference on High-Energy Physics at Rochester* (Interscience Publishers, New York, 1960), p. 185.

† Now at International Business Machines Corporation, Silver Spring, Maryland.
‡ Now at Oxford University, Oxford, England.
§ Now at University of Maryland, College Park, Maryland.

Of course, reactions (2), (3), and (7) were indistinguishable in this experiment.

The elastic and charge exchange interactions have been studied earlier in experiments using scintillation counters as detectors by Glicksman[1] at an incident pion energy of 217 Mev and by Ashkin *et al.*[2] at 220 Mev. In the latter experiment, the elastic scattering differential cross section was reported for eight center-of-mass scattering angles in the range $-0.95 \leqslant \cos\chi_{c.m.} \leqslant 0.80$ ($162.5° \geqslant \chi_{c.m.} \geqslant 37°$) with experimental error on each point of about 9%; however, there was an over-all uncertainty of 5% in the scale of the cross sections. Recent results of further counter experiments have been reported by Goodwin *et al.*,[3] Caris *et al.*,[4] and Kellman.[5]

The threshold for secondary pion production [(5), (6), and (7)] is 170 Mev, and the cross sections for these reactions are small at the incident energy of this experiment. The majority of the experiments to determine the production cross sections have been at energies considerably above the threshold. Perkins *et al.*[6] have measured the $\pi^+$ production cross section at 260 Mev to be $0.14\pm0.10$ mb. Zinov and Korenchenko[7] have measured the quantity $2\sigma(\pi^-+p \rightarrow \pi^-+\pi^++n) + 0.7\sigma(\pi^-+p \rightarrow \pi^-+\pi^0+p)$ at several energies down to 307 Mev. Combining the measurements of Zinov and Korenchenko with the $\pi^+$ production data of Perkins,[6] one finds that the neutral production is probably very small near threshold. Calculations based on the Chew-Low theory[8] predict the ratio of neutral pion production to positive pion production to be greater than 1, and also predict a total pion production cross section much too small to account for the results of Perkins. Rodberg[9] and Goebel[10] have analyzed pion production process assuming a $\pi^-$-$\pi$ interaction, where by introducing suitable scattering lengths for the three isotopic spin states of the pion-pion system, they have succeeded in fitting the data of Perkins.

To summarize, then, this bubble chamber experiment was motivated by the following considerations: (a) The $\pi^-$-$p$ elastic and charge exchange cross sections could be measured by a completely different technique than the counter methods used previously. (b) The elastic differential cross section could be extended to a wider range of scattering angles. (c) The ratio of charge exchange scattering to elastic scattering, which yields information on the isotopic spin state for scattering of the $\pi^-$-$p$ system, could be determined independently of separate normalizing factors; only the relative scanning efficiencies would affect the result. (d) The bremsstrahlung interaction could be observed. (e) The $\pi^+$ and $\pi^0$ [reactions (5) and (6)] production reactions could be detected at an energy close to threshold, utilizing the advantages of a bubble chamber in distinguishing such events.

## EXPERIMENTAL PROCEDURE

### Beam

A beam of negative pions was produced by the 450-Mev proton beam of the Carnegie cyclotron striking an internal beryllium target. The pion beam then passed through two 4-in. aperture quadrupole focusing magnets, through the 12-ft shielding wall, a momentum selecting magnet which bent the beam through 40°, and the external field of the bubble chamber magnet, before entering the chamber. A polyethylene bag filled with helium and extending from the cyclotron window to the deflecting magnet was used and yielded ~15% increase in beam intensity. The beam energy at the center of the chamber was determined from an integral range curve and from curvature measurements on the tracks to be $(224\pm6)$ Mev. The momentum spectrum from curvature measurements on tracks traversing the full chamber length is shown in Fig. 1. The main contributions to the width of the distribution arose from multiple Coulomb scattering of the pions and from the finite precision of curvature measurements. The beam contamination was estimated from the range curve and from a pulse-height analysis using a Čerenkov counter in a very similar beam[5] to be $(5\pm2)$% muons and $(1\pm1)$% electrons. The full cyclotron beam intensity was used, yielding about 7 tracks per picture.

### Chamber

The pion beam traversed a cylindrical liquid hydrogen bubble chamber of diameter 15.2 cm and depth 7.6 cm which has been described elsewhere.[11] The magnetic field was $13.10\pm0.06$ kgauss at the center of the chamber and was spatially constant to within $\frac{1}{2}$% over the volume occupied by the chamber. During ~100 hr of chamber operation, 79 000 pictures were taken, of which 61 000 ultimately were used.

[1] M. Glickman, Phys. Rev. **94**, 1335 (1954).
[2] J. Ashkin, J. P. Blaser, F. Feiner, and M. O. Stern, Phys. Rev. **105**, 724 (1957).
[3] L. H. Goodwin, University of California Radiation Laboratory Report UCRL-9119, 1960 (unpublished); J. Caris, L. Goodwin, R. Kenney, and V. Perez-Mendez, Phys. Rev. **122**, 262 (1961).
[4] J. C. Caris, University of California Radiation Laboratory Report UCRL-9048, 1960 (unpublished); J. Caris, R. Kenney and V. Perez-Mendez, Phys. Rev. **122**, 655 (1961); J. Caris, R. Kenney, V. Perez-Mendez, and W. Perkins, *ibid.* **121**, 893 (1961).
[5] S. Kellman, thesis, Carnegie Institute of Technology, 1961 (unpublished).
[6] W. Perkins, University of California Radiation Laboratory Report UCRL-8778, 1959 (unpublished); W. Perkins, J. Caris, R. Kenney, and V. Perez-Mendez, Phys. Rev. **118**, 1364 (1960); W. Perkins, J. Caris, R. Kenney, E. Knapp, and V. Perez-Mendez, Phys. Rev. Letters **3**, 56 (1959).
[7] V. Zinov and S. Korenchenko, Soviet Phys.-JETP **34**, 210 (1958).
[8] S. Barshay, Phys. Rev. **103**, 1102 (1956); J. Franklin, *ibid.* **105**, 1101 (1957); E. Kazes, *ibid.* **106**, 1090 (1957).
[9] L. S. Rodberg, Phys. Rev. Letters **3**, 58 (1959).
[10] C. Goebel, Phys. Rev. Letters **1**, 337 (1958).
[11] Bubble chamber description—M. Derrick, J. G. Fetkovich, T. H. Fields, and J. Deahl, Phys. Rev. **120**, 1022 (1960).

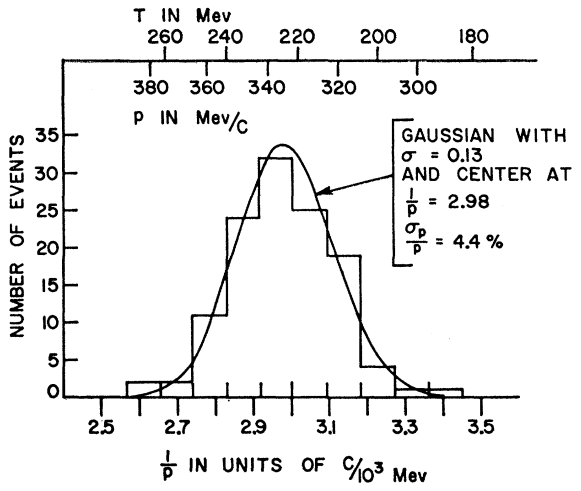


FIG. 1. The momentum spectrum of the incident beam from curvature measurements.

## Scanning

The photographs were scanned using three distinct scanning procedures: (a) an event scan, (b) a track count, and (c) a search for charge exchange endings.

### (*a*) *Event Scan*

In the event scanning, three general types of interactions were sought; those with zero, one, or two outgoing prongs from an incident track of negative curvature. The zero-prong events were either genuine interactions in the liquid or were caused by a beam particle entering one of the glass windows of the chamber. The one-prong events were small-angle scatterings in which the recoil particle was too short to be visible. Two-prong events could be elastic scatterings, bremsstrahlung events, pion production [reactions (5) and (6)], or one of the reactions leading to uncharged final state where an internal electron pair was created. Occurrences exhibiting unusual features or not falling into these categories were reported as "strange." Each event reported as a result of this scan was then examined by a physicist in order to eliminate false events such as chance coincidences, and to initially classify the event for measurement purposes.

### (*b*) *Track Count*

A measurement of the incident flux was required in order to calculate absolute cross sections. For this reason, a track count was carried out as follows: On every tenth frame on each roll of film all negative tracks falling within 20° of the average incident beam direction and satisfying the other entrance area criteria (discussed below) were counted, regardless of subsequent interaction. In addition to track counting, every frame was examined and classified as acceptable or unscannable (because of none or too many tracks, or poor picture quality). In this manner, all scans and track counts were made consistent with respect to the frames actually used for data.

### (*c*) *Charge Exchange Scan*

Although zero-prong events were recorded during the initial event scan, subsequent comparison scans indicated that the efficiency of finding endings was lower than that for other events. For this reason, a separate scan for track endings was performed on ~40% of the film by two of the best scanners. The results of this scan were combined with those endings found on the initial event scan for the final analysis.

Definition of an entrance region was required for these three procedures since it was desired to consider only incident tracks which had entered through a thin copper window in the chamber body. This entrance criterion was applied while track counting and on the charge endings by the scanners through construction of a template using the fiducial marks etched on the glass windows for reference. Other events were checked against this same entrance criterion by a computer calculation.

## Measuring

A digitized measuring projector[12,13] was used to measure the Cartesian coordinates of appropriate points in the pictures. Measurements on tracks in this experiment with this device were found to be reproducible to about 7 $\mu$ on the film (the chamber to film demagnification was 6). The measurements taken for each view of an event included three fiducial marks, three evenly spaced points on each track of the interaction, and a remeasurement of one fiducial to permit a computer check for digitizer errors or film slippage during measurement. Events which were obviously inelastic were measured at five points on each track so as to carry out an accurate momentum analysis.

The coordinates of the vertex and the space angles of all 2-prong and 1-prong events were calculated on an IBM 650 computer. In addition, for 2-prong inelastic events the momentum of each track was calculated.

# DATA PROCESSING

## Useful Chamber Volume

In order to eliminate scanning inefficiencies caused by the difficulty of finding events near a boundary of the chamber, each event vertex was required to lie within a central volume of depth 5.2 cm and length in the beam direction of 10.4 cm. The width of the volume was

[12] M. Derrick, T. H. Fields, and R. Findley, *Proceedings of the International Conference on High-Energy Accelerators and Instrumentation, CERN* (European Organization for Nuclear Research, Geneva, 1959), Session 6.

[13] T. Fields and R. Findley, Rev. Sci. Instr. **31**, 1312 (1960).

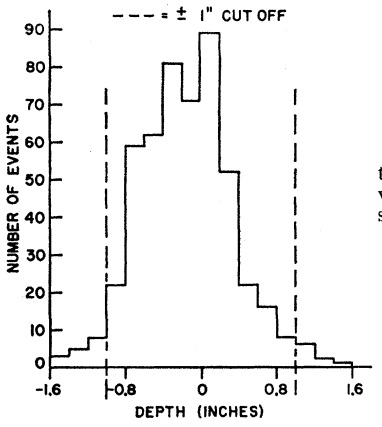


FIG. 2. The distribution in depth of vertices of elastic scattering events.

fixed only by the entrance criterion. The distribution in depth of elastic scatterings is shown in Fig. 2

## Elastic Events

Elastic scatterings were identified by using the kinematic correlation between the pion scattering angle and the recoil proton angle as well as the degree of coplanarity of the events. The kinematic angular correlation for 50 typical elastic events is shown in Fig. 3. Events which initially failed to satisfy the angular correlation within errors were remeasured. Those events which lay off the kinematic curve for two measurements were then measured and computed as inelastic events. The final plot of the deviations from the kinematic line for all elastic events showed a standard deviation of 0.9°. The coplanarity function was defined as the volume of the parallelepiped of unit sides formed by the three particle directions. All events classified as elastic satisfied the coplanarity criterion within the measurement errors.

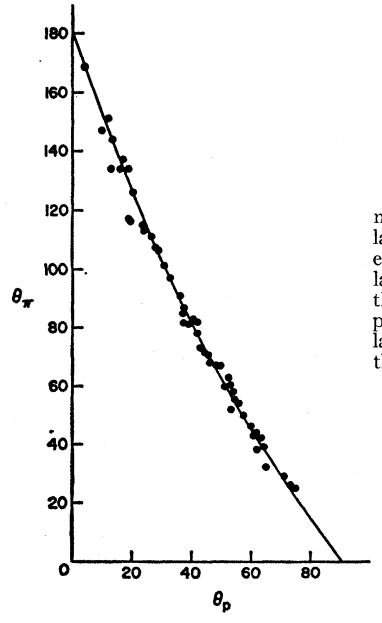


FIG. 3. The kinematic angular correlation for 50 typical elastic events. The laboratory angle of the scattered pion is plotted against the laboratory angle of the recoil proton.

The efficiency of finding elastic scatterings was checked by comparing scans of the same film by two different scanners, and by plotting azimuthal distributions of the scattering plane. The film was scanned about $2\frac{1}{4}$ times, and the comparison of the scans indicated an elastic event net scanning inefficiency of about 1%. The azimuthal distributions for various scattering angle intervals (Fig. 4) appeared to be isotropic except for the extreme backward direction ($153.0° < \chi_{c.m.} < 180°$) where a slight loss of steep events ($75° < \Phi < 90°$) was indicated. A 14-event efficiency correction was added in this interval, representing a 0.9% correction to the total number of events. The final azimuthal distribution including this efficiency correction is shown in Fig. 5.

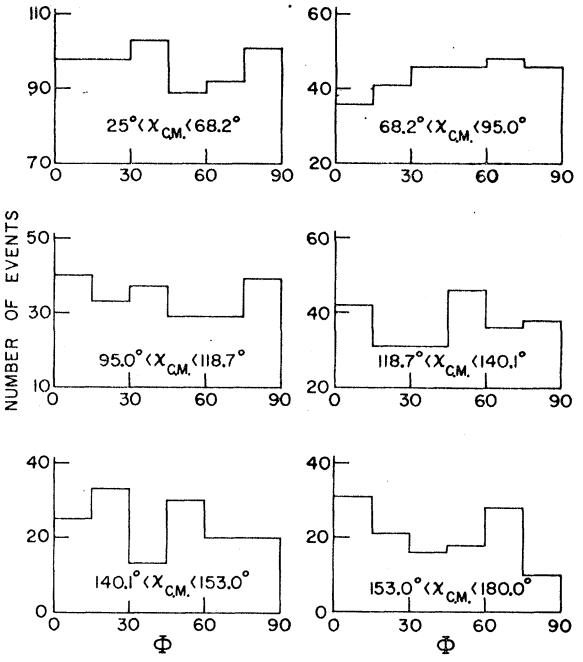


FIG. 4. The azimuthal distributions for various angular intervals of the c.m. scattering angle of the pion.

## Inelastic Events

All events which were obviously inelastic or which failed to meet the criteria for elastic scatterings were computed as inelastic. An IBM 650 computer program calculated the mass of the unseen neutral particle successively assuming the positive outgoing particle to be a pion or a proton. Also, the ranges of both outgoing visible particles were calculated under the two assumptions. The results of this calculation were analyzed in conjunction with a visual inspection of a print of each event. The constraints of energy and momentum conservation provided limitations on the available lab momentum as a function of laboratory scattering angle

for both outgoing pions and the recoil nucleon. Events yielding a null mass for the neutral particle were classified as bremsstrahlung if the deviation from the elastic kinematic fit curve was greater than 5°.

### Track Length Correction

The distribution in depth of the incident beam was assumed to be the same as that of the charge exchange events vertices (Fig. 6) since those events were endings, and no loss of efficiency near the windows of the chamber was anticipated. The depth distribution of elastic scatterings was consistent with that of endings, indicating no loss of those events within the depth cutoff. The fraction of tracks within the depth cutoff of $\pm 2.54$ cm was $(93.2\pm 2.5)\%$.

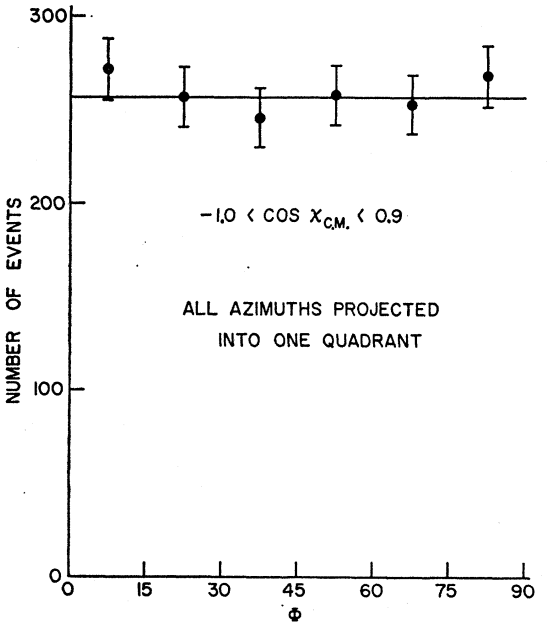


FIG. 5. The final azimuthal distribution for all events, including an efficiency correction of 14 events for loss of steep events (see text).

The reduction in total track length due to interactions was estimated from the previously determined[2] total cross section, and amounted to 0.7%.

## RESULTS

### Elastic Scatterings

The azimuthal distribution plots of elastic scatterings for various scattering angles indicated no loss of small-angle events for c.m. angles larger than 25°. The angular distribution of the 1570 elastic scattering events was corrected for the Coulomb interaction by using the Fermi (i) phase shifts of Ashkin[2] by the method described in Ashkin *et al.*[14] and Solmitz.[15] The consistency of the procedure is indicated by the fact that the final phase shifts found from the present data agree within errors with those assumed for the Coulomb correction. Table I gives the differential cross section of the observed elastic events and the Coulomb interaction corrections. The statistical errors plus a conservative estimate of the error in the efficiency correction of the point at $\cos\chi_{c.m.}=0.95$ are included. A least-squares fit to the corrected data was computed assuming a form $d\sigma/d\Omega=A_0+A_1\cos\chi_{c.m.}+A_2\cos^2\chi_{c.m.}$. This fit is plotted with the corrected data in Fig. 7. The coefficients obtained are included in Table II. The $\chi^2$ test parameter of this fit was $M=7$ with expectation value 15. Thus, there was no evidence for a $\cos^3\chi$ term in the angular distribution, within the accuracy of this experiment.

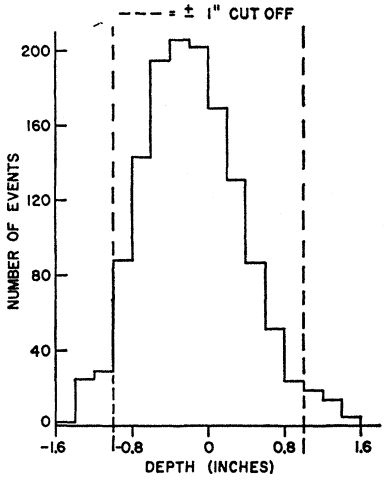


FIG. 6. The depth distribution of charge exchange events.

The total elastic cross section was obtained by integration of the angular distribution over the entire range of the center-of-mass angle, yielding $\sigma_{\text{elastic}} = (16.0\pm 0.8)$ mb, as shown in Table II.

TABLE I. Elastic scattering angular distribution results.

| $\chi_{c.m.}$ (deg) | $\cos\chi_{c.m.}$ | $d\sigma/d\Omega$ (uncorrected) (mb/sr) | Coulomb correction (mb/sr) | $d\sigma/d\Omega$ (corrected) (mb/sr) |
|---|---|---|---|---|
| 161.8 | −0.95 | 2.02±0.25 | −0.02 | 2.00±0.25 |
| 148.2 | −0.85 | 1.69±0.16 | −0.02 | 1.67±0.16 |
| 138.6 | −0.75 | 1.41±0.15 | −0.02 | 1.39±0.15 |
| 130.5 | −0.65 | 1.14±0.13 | −0.02 | 1.12±0.13 |
| 123.3 | −0.55 | 0.91±0.12 | −0.02 | 0.89±0.12 |
| 116.8 | −0.45 | 0.97±0.13 | −0.02 | 0.95±0.13 |
| 110.5 | −0.35 | 0.73±0.11 | −0.02 | 0.71±0.11 |
| 104.5 | −0.25 | 0.64±0.10 | −0.02 | 0.62±0.10 |
| 98.6 | −0.15 | 0.75±0.11 | −0.01 | 0.74±0.11 |
| 92.9 | −0.05 | 0.68±0.11 | −0.01 | 0.67±0.11 |
| 87.1 | 0.05 | 0.72±0.11 | −0.01 | 0.71±0.11 |
| 81.4 | 0.15 | 0.60±0.10 | −0.01 | 0.59±0.10 |
| 75.5 | 0.25 | 0.91±0.12 | 0 | 0.91±0.12 |
| 69.5 | 0.35 | 0.94±0.12 | 0 | 0.94±0.12 |
| 63.2 | 0.45 | 1.29±0.14 | 0.01 | 1.30±0.14 |
| 56.6 | 0.55 | 1.35±0.15 | 0.01 | 1.36±0.15 |
| 49.4 | 0.65 | 1.48±0.15 | 0.02 | 1.50±0.15 |
| 41.4 | 0.75 | 1.89±0.18 | 0.05 | 1.94±0.18 |
| 31.8 | 0.85 | 1.95±0.18 | 0.09 | 2.04±0.18 |

[14] J. Ashkin, J. P. Blaser, F. Feiner, and M. O. Stern, Phys. Rev. **101**, 1149 (1956).
[15] F. T. Solmitz, Phys. Rev. **94**, 1799 (1954).

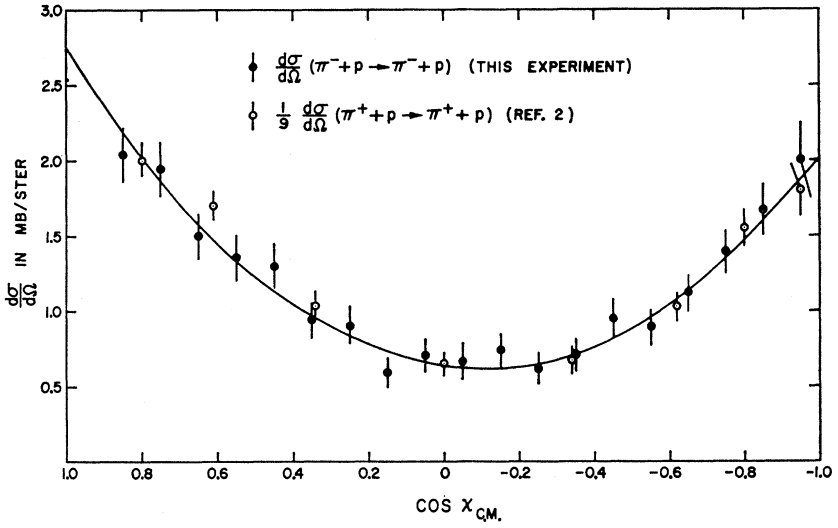


FIG. 7. The center-of-mass angular distribution for elastic scatterings. The solid curve is a least-squares fit to the data assuming an angular distribution of the form $d\sigma/d\Omega=A_0+A_1\cos\chi_{c.m.}+A_2\cos^2\chi_{c.m.}$.

## Charge Exchange

The charge exchange total cross section was found by adding the Dalitz electron-pair events to the endings in the liquid. Only ~40% of the film was used for the charge exchange cross section. The result was 34.4±1.9 mb, including a 6±2% efficiency correction indicated by comparing results from the three scans. A 0.6-mb correction for the $\pi^-+p\to\gamma+n$ cross section was subtracted from the observed result to yield this cross section. On the basis of this cross section, the number of internal electron pairs expected in all of the film was 44 which is in satisfactory agreement with the 40 pairs observed.

For several hundred of the charge exchange events, the curvature of the incident tracks was measured with a template, in order to guard against spurious events caused by occasional low-energy pions coming to rest in the hydrogen. No such spurious events were observed.

TABLE II. Results.

| Process | Total cross section | Number of events |
|---|---|---|
| $\pi^-+p\to\pi^-+p$ | 16.0±0.8 mb | 1570 |
| $\pi^-+p\to\pi^-+p+\gamma$ | 0.040 mb (empirical gamma lab energy cutoff=50 Mev) | 4 |
| $\pi^-+p\to\pi^0+n$ | 34.4±1.9 mb | 1210[a] |
| $\pi^-+p\to\gamma+n$ | 0.6 mb (from detailed balancing) | 17[a] (estimated from 0.6 mb cross section) |
| $\pi^-+p\to\pi^-+\pi^++n$ | 0.03±0.02 mb | 3 |
| $\pi^-+p\to\pi^-+\pi^0+p$ | 0 | 0 |
| Total | 50.5±1.9 mb (not including $\pi^-+p\to\gamma+n$ cross section) | |

Elastic differential cross section (after Coulomb correction)

$d\sigma/d\Omega=(0.70\pm0.04)+(0.33\pm0.07)\cos\chi_{c.m.}+(1.69\pm0.13)\cos^2\chi_{c.m.}$,

where the coefficients are in mb/sr; the angular range $25°<\chi_{c.m.}<+180°$ was used in obtaining this fit.

Dalitz electron pairs

$\pi^-+p\to\pi^0+n\to e^+e^-+\gamma+n$

Predicted 44
Observed 40 } includes all film scanned

Dispersion curve

$D_-{}^b(0)/\lambda\!\!\!^{-}_c=-0.07_{-0.06}{}^{+0.07}$ using $d\sigma/d\Omega(0)=(2.72\pm0.15)\times10^{-27}$ cm², where $\lambda\!\!\!^{-}_c$ is the Compton wavelength of the pion.

[a] based on 150 000 incident tracks. The other numbers represent 360 000 incident tracks.

## Bremsstrahlung

Four inelastic events were classified as radiative scatterings since the calculated neutral mass value was consistent with zero, and inconsistent with alternative interpretations of those events. They were separated from the elastic events by the kinematic correlation criteria. The cutoff in those criteria was required by measuring errors and was sufficiently broad to include some bremsstrahlung events with the elastic scatterings. The accuracy of the elastic scattering criteria corresponded to a minimum detectable $\gamma$-ray energy of about 50 Mev. For such radiative events a cross section of 0.04 mb was obtained. This value is in agreement within its large uncertainty with the theoretical cross section which was calculated by Cutkosky.[16]

## Pion Production

Analysis of all inelastic events yielded 3 events of type (5) and none of type (6). Two of these $\pi^+$ production events were also identified by the stopping and subsequent $\pi^+\to\mu$ decay of the positive pion in the chamber. One event was classified as either an electron pair or a $\pi^+$ production. However, momentum-angle considerations excluded the $\pi^0$ production possibility. The resulting $\pi^+$ production cross section was 0.03±0.02 mb.

[16] R. E. Cutkosky, Phys. Rev. 113, 727 (1959); and private communication.

TABLE III. Summary of various experimental results.

| Process | Ashkin[a] | Kellman[b] | This experiment | Goodwin[c] | Caris[d] | Zinov[e] | Units |
|---|---|---|---|---|---|---|---|
| Energy | 220±7 | 226±8 | 224±10 | 230±8 | 230±8 | 240±7 | Mev |
| $\pi^-+p\rightarrow\pi^-+p$ | 19.5±0.6 | 17.4±0.3 | 16.0±0.8 | 20.8±0.4 | ··· | 16.1±0.6 | mb |
| $\pi^-+p\rightarrow\pi^0+n$ | 33.3±0.7 | ··· | 34.4±1.9 | ··· | 30.4±1.3 | 32.2±1.4 | mb |
| $\sigma_{\text{Total}}$(less $\sigma_{\gamma n}$) | 53.2±1.5 | 52.9±1.4 | 50.5±2.1 | 48±2[f] | ··· | 48.3±3.3 | mb |
| $A_0$[g] | 0.86±0.06 | 0.66±0.02 | 0.70±0.04 | 0.95±0.04 | ··· | 0.81±0.08 | mb/sr |
| $A_1$[g] | 0.30±0.08 | 0.41±0.05 | 0.33±0.07 | 0.55±0.06 | ··· | 0.23±0.09 | mb/sr |
| $A_2$[g] | 2.07±0.18 | 2.16±0.08 | 1.69±0.13 | 2.10±0.09 | ··· | 1.41±0.18 | mb/sr |
| $\frac{\sigma(\text{charge exchange})}{\sigma(\text{elastic})}$ | 1.71±0.06 | 2.04±0.09 | 2.15±0.09 | 1.31±0.10 | 1.55±0.07 | 2.00±0.11 | |

[a] See reference 2.
[b] See reference 5.
[c] See reference 3.
[d] See reference 4.
[e] See reference 7.
[f] From data of Pontecorvo.
[g] $d\sigma(\pi^-+p\rightarrow\pi^-+p)/d\Omega=A_0+A_1\cos\chi_{\text{c.m.}}+A_2\cos^2\chi_{\text{c.m.}}$.

## Total Cross Section

The total cross section was calculated by summing the cross sections for each reaction. The result obtained was 50.5±1.9 mb for the purely nuclear cross section which is in excellent agreement with the counter transmission experiments of Pontecorvo.[17]

## DISCUSSION

### Cross Sections

In Table III are shown the results of several experiments on $\pi^-$-$p$ scattering in the energy range 220–240 Mev. Although the total cross sections are in good agreement, the ratio of charge exchange to elastic cross sections varied markedly, far outside the quoted experimental errors. The present experiment agrees well with that of Zinov[18] with respect to this ratio and with respect to the angular distribution. The angular distribution also agrees fairly well with that reported by Ashkin, but the present elastic cross section is about 18% smaller. If the scattering is considered in terms of the two possible isotopic spin states, $T=\frac{1}{2}$ and $T=\frac{3}{2}$, pion-proton scattering amplitudes consist of the following combinations:

$$\pi^++p\rightarrow\pi^++p,\quad f=f_3,$$
$$\pi^-+p\rightarrow\pi^0+n,\quad f=\tfrac{1}{3}\sqrt{2}(-f_1+f_3),$$
$$\pi^-+p\rightarrow\pi^-+p,\quad f=\tfrac{1}{3}(2f_1+f_3),$$

where $f_{2T}$ denotes the scattering amplitude for the state with total isotopic spin $T$.[19] If the $T=\frac{3}{2}$ state is much more important than the $T=\frac{1}{2}$ state for these pion energies, then one expects the ratio,

$$\frac{\sigma(\text{charge exchange})}{\sigma(\text{elastic})}=\frac{2|-f_1+f_3|^2}{|2f_1+f_3|^2},$$

to be approximately 2. The value measured in this experiment is 2.15±0.09, and was independent of the track count procedure, and of the beam contamination of muons and electrons. The last row of Table III shows the value of this ratio as measured by different experimenters. The values reported by Goodwin *et al.*,[3] and Caris *et al.*[4] are much lower than the value measured in the present experiment. Regarding this disagreement we may point out that when Kellman[5] repeated the counter experiment of Ashkin *et al.*[2] at 220 Mev, taking special precautions to account for electrons in the counter telescope measuring the scattered pions, the new value of the total cross section for elastic scattering was reduced by ~11%. This changed their ratio of charge exchange to elastic scattering from 1.71±0.06 to 2.04±0.09, bringing it into good agreement with our value. So it is possible that there was some systematic error in the Berkeley[3,4] experiments due to electrons which could account for this difference. The dominance of the $T=\frac{3}{2}$ state in the scattering reactions is further indicated by the excellent agreement of $\frac{1}{9}(d\sigma/d\Omega)(\pi^++p\rightarrow\pi^++p)$ determined by Ashkin[2] and $(d\sigma/d\Omega)(\pi^-+p\rightarrow\pi^-+p)$ from this experiment as shown in Fig. 7.

The present angular distribution yields a value for $D_-{}^b$ (the real part of the forward scattering amplitude) which is in good agreement with the dispersion curve as given by Cronin.[20] However, the error is large, as Fig. 8 shows.

### Phase-Shift Analysis

The angular distribution of the elastic scattering and the charge exchange total cross section were used in conjunction with the $\pi^+$-$p$ elastic scattering differential cross section of Ashkin[2] and the recoil proton polarization results of Kunze[21] as the data for a phase-shift analysis. A program was written for the IBM 650 to minimize the error function $M=\sum(\epsilon_i)^2$, where $\epsilon_i$ represents the difference between the experimentally

[17] B. Pontecorvo, *Ninth Annual International Conference on High-Energy Physics at Kiev, 1959* (Academy of Science, U.S.S.R., 1961). Report by B. Pontecorvo on Pion-Nucleon Interaction.
[18] V. G. Zinov and S. M. Korenchenko, Soviet Physics—JETP **36**, 428 (1959).
[19] J. D. Jackson, *The Physics of Elementary Particles* (Princeton University Press, Princeton, New Jersey, 1958), p. 12.
[20] J. W. Cronin, Phys. Rev. **118**, 824 (1960).
[21] J. Kunze, T. Romanowski, J. Ashkin, and A. Burger, Phys. Rev. **117**, 859 (1960).

TABLE IV. Phase-shift results.[a]

| Type | $M$ | $\alpha_1$ | $\alpha_{11}$ | $\alpha_{13}$ | $\alpha_3$ | $\alpha_{31}$ | $\alpha_{33}$ |
|---|---|---|---|---|---|---|---|
| Fermi (i) | 7.6 | 14.8±3.5 | 5.9±4.5 | 0±2.0 | −15.5±3.5 | −2.1±5.5 | 112.3±3.0 |
| Yang (ii) | 10.1 | −10.3±2.0 | 4.6±2.0 | 9.0±1.5 | −16.3±3.0 | 258.4±4.5 | 143.3±1.5 |
| Fermi (ii) | 12.9 | −2.7±2.0 | −4.3±2.5 | 9.8±1.0 | −16.1±2.0 | −1.5±3.5 | 112.3±1.0 |

[a] The $2T$, $2j$ subscript notation is the standard one. Phase shifts are given in degrees.

determined value of a quantity and the value computed from the phase shifts, as measured in units of the experimental errors of the quantity. Nineteen data values were used to obtain the six $s$, $p$ phase shifts yielding an expectation value for $M$ of 13. As starting values for the phase shifts, the four graphical sets obtained by Ashkin,[2] five variations of these, and five random sets were used. The best fit was found in a Fermi (i) set; this solution was found several times, including once from a random starting set. However, the two other sets, a Fermi (ii) and a Yang (ii) type were determined with statistically satisfactory fits. The numerical results are shown in Table IV. The recoil polarization data of Kunze *et al.*[21] are thus seen to be inadequate criteria for the exclusion of the Yang (ii) type phase shifts. Note that, although there exists a large discrepancy between the ratio $\sigma$(charge exchange)/$\sigma$(elastic) as measured by Ashkin *et al.*[2] and in this experiment, the present phase shifts are hardly changed from those obtained previously.

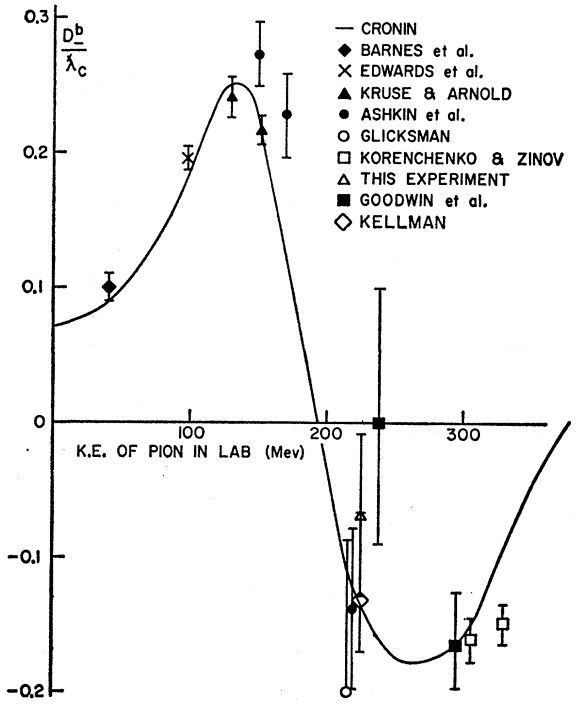


FIG. 8. The real part of the forward scattering amplitude as a function of energy.

## Pion Production Results

At 220 Mev it is reasonable to assume that the two pions are in a relative $s$ state. Then the possible isotopic spin of the two-pion system can be 0 or 2. It is clear that the $(\pi^-\pi^0)$ state can arise only via $T_{2\pi}=2$. Thus the experimental result of production ratio of $\pi^0/\pi^+$ = (0 events)/(3 events) indicates that production process occurs via the $T_{2\pi}=0$ state, and thus from the $T_{\pi^-p}=\frac{1}{2}$ initial state. If it is assumed that production takes place from a $T_{\pi^-p}=\frac{3}{2}$ initial state, which yields the $T_{2\pi}=2$ state of the $s$-wave 2-pion system, one obtains a ratio of $\pi^0/\pi^+=9/2$, in rather definite disagreement with the observed ratio. This conclusion that the $T_{2\pi}=0$ state is dominant if the production process proceeds via $\pi$-$\pi$ interaction in a relative $s$ state is in accord with several recent experimental and theoretical results[22–25] but the number of events obtained is too small to allow a more quantitative analysis.

### ACKNOWLEDGMENTS

We wish to thank James Thompson, Homer Collins, and the operating personnel of the Carnegie Tech cyclotron for substantial aid in performing the bubble chamber exposure. The efficient scanning done by Betty Cherry, Donna Stasak, Steve Stasak, Joe Rudman, and others, is gratefully acknowledged. We also wish to thank Gale Pewitt and Robert McIlwain for assistance in both the run and the data reduction.

[22] B. R. Desai, Phys. Rev. Letters **6**, 497 (1961).
[23] A. Abashian, N. Booth, and K. Crowe, Phys. Rev. Letters **5**, 268 (1960).
[24] P. Carruthers and H. A. Bethe, Phys. Rev. Letters **4**, 536 (1960).
[25] C. J. Goebel and H. J. Schnitzer, Phys. Rev. **123**, 1021 (1961).